EXPERIMENTAL AND COMPUTATIONAL TESTS INVOLVING R-11, R-19, AND R-30 FIBERGLASS INSULATIONS

K.T. Harris[+], T.A. McCarty[*], J.A. Roux[#]
Department of Mechanical Engineering
University of Mississippi
University, MS 38677

ABSTRACT

The attic regions of residential dwellings are important areas with respect to energy conservation. The primary objective of this study is to determine the effective changes in total heat transfer due to varying the attic insulation thickness from R-11 to R-19 to R-30 and also due to the addition of horizontally installed radiant barriers (for R-30). Experimental data (including winter and summer) were collected at an occupied north Mississippi residence and various profiles such as time histories of temperature, heat flux, and vapor water concentrations are presented to support the experimentally determined effects on the overall heat transfer. A transient, one-dimensional, computational thermal model that incorporates combined conduction and radiation heat transfer and moisture transport is also used to predict the changes in the total heat flux. These predictions are then compared with the experimental results for typical summer and winter days for north Mississippi.

Key Words: heat-flux, adsorption/desorption, concentration-gradient, computational model, radiant barrier, conduction, radiation, mass transport.

[+]Graduate Student; [*]Assistant Professor; [#]Professor

INTRODUCTION

Energy conservation in residential dwellings has become an extremely important issue in today's society. It has been well documented [1-4] that one of the major problem areas in these dwellings are their attics where considerable amounts of energy can be lost or gained depending on the climatic conditions of winter or summer. The basic objective was to determine the effective changes in the total heat transfer (radiation, conduction, and contributions of the mass transfer) as a result of variations in fiberglass insulation thickness as well as the addition of horizontal radiant barriers (for R-30 only). The goals of this investigation were accomplished by two means: 1) measurements of temperature, heat flux, and relative humidity and 2) computer simulations using a computational heat transfer model. In this study, three levels of thermal resistance were considered: R-11 at thickness 0.089 m (3.50 inches), R-19 at thickness 0.159 m (6.25 inches), and R-30 at thickness 0.248 m (9.75 inches).

In this study, heat flux, temperature, and relative humidity were measured in an occupied residence located in north Mississippi. These data were collected during the winter, spring, and summer and were employed to assess the effective changes in the total heat transfer. The computational tool used in this study is a transient, one-dimensional model. The model has been developed over the past several years by Gorthala, Harris, et al.[2,3,4]. The governing equations for the model are the energy equation, the radiative transport equation, and the mass transport equations for liquid (i.e. water that is adsorbed into the fibers) water and vapor water. The energy equation includes the transport of energy due to one-dimensional conduction, radiation heat transport, diffusion of vapor and liquid water, and a source/sink term simulating the adsorption/desorption of water. The radiative transport equation describes the intensity field;

this includes the volumetrically adsorbed intensity, the volumetrically scattered intensity, and the volumetrically emitted intensity. The radiative intensity field must be determined in order to evaluate the radiative heat flux term in the energy equation. There are two moisture transport equations, one for the liquid and one for the vapor. The liquid water is considered to be transported through the fibers, but only slightly, due to the fact that the mass conductivity coefficient for liquid water is extremely low ($\approx 10^{-9}$). Also, there is a source/sink depending on whether the fibers are losing or gaining water. Similar statements can be made for the vapor transport equation; however the mass conductivity for vapor water is higher ($\approx 10^{-5}$).

A series of heat transfer measurements in attic insulations have been performed at the Oak Ridge National Laboratory (ORNL). The first experiment [5] consisted of tests to determine the magnitude of heat flux (W/m^2) reduction when radiant barriers were installed in the attics of unoccupied single-family houses insulated with R-19 fiberglass insulation. The results for summer conditions showed a reduction of about 39% in measured peak ceiling heat fluxes when the radiant barrier was laid horizontally on top of the fiberglass insulation. It was also found that the 7-day time-integrated-heat-flux (kJ/m^2) through the ceiling with the horizontal mounted barriers were 35% lower than the case of no radiant barrier and 30% lower with the use of mounting the radiant barriers on the wooden, sloping truss members of the roof's attic (i.e. truss-mounted). By truss mounted it is meant that the radiant barrier is attached to the bottom of the wooden roof rafters. This places the radiant barrier some distance from the fiberglass insulation; as opposed to the horizontally mounted radiant barrier which is laid on the top of the insulation.

The second set of tests [6] for R-19 insulation only was conducted in the winter of 1985-

86 to determine the magnitude of the peak ceiling heat flux reduction achieved by the installation of truss and horizontal mounted radiant barriers. These experiments were conducted at two identically configured side-by-side test houses; the only difference was that one had a radiant barrier installed in the attic and the other did not. The results indicated that there was no significant change in ceiling heat flux caused by the addition of radiant barriers.

Finally, a third experiment [7] was conducted in the winter of 1986-87 to establish the heating energy performance of R-11 and R-30 fiberglass attic insulations in combination with truss and horizontally installed radiant barriers. The results showed that the horizontal radiant barrier used with R-11 attic insulation reduced the attic heat flux by 19% as compared with R-11 with no radiant barrier and the truss mounted barrier showed a reduction of about 8% in the ceiling heat flux. The R-30 attic insulation with the horizontal radiant barrier showed an attic heat flux reduction of about 9.5% as compared with R-30 with no radiant barrier and the truss mounted barrier showed a reduction close to 4% in the ceiling heat flux.

This paper is a companion paper to two previous publications [3,4]. However, it is different in that [3] contained only predicted results for R-11 and R-30 insulations ; whereas, this paper will contain measured and predicted results for R-11 and R-30 (R-30 with and without a radiant barrier). This present paper is likewise different in that [4] only considered moisture effects for R-19. Thus, this paper will give better insight into understanding of the effects of moisture and radiant barriers for R-11, R-19, and R-30 insulations.

EXPERIMENTAL SETUP

Shown in Fig. 1 is a typical attic sketch for a residential home with insulation. The boundaries of the insulation batt are air at the top and gypsum board (sheetrock .0127m) on the

house ceiling which is at the bottom of the insulation batt. The subscripts s, o, a, and r represent substrate (bottom of the insulation batt), insulation top, attic air, and roof respectively. Also it should be noted that the coordinate system originates at the substrate (fiberglass/sheetrock interface) where $y=0$ and hence at the top of the insulation batt $y=y_o$.

The residential home where the data were recorded is occupied and is located in the northern part of the state of Mississippi. Temperature, heat flux, and relative humidity data were collected for horizontally oriented fiberglass insulations. The thermal data were recorded every 15 minutes using an HP 3528A data acquisition system. Temperatures (see Fig. 2) were measured with type-J thermocouples that are stated to be accurate to $\pm 1/4$ K. Relative humidities were measured with Hycal CT-829-A-RX temperature compensated relative humidity (R.H.) meters (see Fig. 2) that are accurate to less than 1% between $20 < R.H. < 80\%$. Heat fluxes were measured with the Hycal BI-7-20-WP-J-X-X6 high sensitivity heat flux meters (see Fig. 2); the heat flux meters were calibrated by Holometrix Inc. and are stated to be accurate to $\pm 5\%$ of full scale (heat flux of 7.8 W/m^2). The heat flux meters were located at the interface between the fiberglass batt and gypsum board at the substrate.

COMPUTATIONAL MODEL

The basic equations for the computational model are the energy equation, the moisture transport equations, and the radiative transport equation. To simplify the model, the attic insulation is considered to behave like a plane parallel layer and the primary assumptions are given as follows: 1) transient, one-dimensional combined conduction, radiation heat transfer with water vapor diffusion, and adsorption/desorption of moisture; 2) the fiberglass insulation was considered to be a radiative absorbing, emitting and scattering (isotropic) medium; 3) gray

radiative properties (extinction coefficient and albedo); 4) convection is neglected; 5) relative humidities and temperatures at the boundaries are known (measured) functions of time.

This work also considers both adsorption and desorption of water vapor to be described by the same heat of vaporization [8,9] and it neglects any hysteresis phenomenon that may be present between the adsorption and desorption isotherms. The density of the fiberglass insulation was measured to be 12 kg/m^3 [10]. The temperatures at the insulation top, bottom, and roof are the required boundary condition information for solving the energy equation and the radiative transport equation. The boundary temperatures and relative humidities are required for obtaining concentrations of liquid water and vapor water which are needed for solving the moisture transport equations. Emissivities are specified at the roof ($\epsilon_n = 1, \rho_n = .85$) and substrate ($\epsilon_s = 1, \rho_s = .93$) surfaces [11]. That thermal/radiative properties used in this model are presented in Table 1.

Energy Equation

The one-dimensional energy equation for transient, conduction, radiation heat transport, diffusion of vapor and liquid water and phase change (adsorption/desorption) is given by

$$\frac{\partial}{\partial y}\left[k_f \frac{\partial T}{\partial y}\right] - \frac{\partial q_r}{\partial y} + \frac{\partial}{\partial y}\left[\gamma_v \, i_v \, \frac{\partial m_v}{\partial y}\right] + \frac{\partial}{\partial y}\left[\gamma_b \, i_b \frac{\partial m_b}{\partial y}\right] + \dot{q} = \rho_f c_f \frac{\partial T}{\partial t} \qquad (1)$$

with

$$\dot{q} = h_{ad} \dot{m}_b \qquad (1a)$$

and where k_f is the bulk thermal conductivity of the insulation given by Houston [12], ρ_f is the bulk density of the insulation [10], c_f is the specific heat of the insulation [10]. The symbols γ_b

and γ_v are the moisture conductivity coefficients; i_b and i_v are the specific enthalpies of the liquid and vapor, respectively; h_{ad} (Eq. (1a)) is the heat of water adsorption/desorption; m_b (kg/m^3) is the liquid water concentration; m_v (kg/m^3) is the vapor water concentration; q_r is the radiative heat flux; and $\dot{m}_b$ is defined as the rate of adsorption/desorption of water (sink/source term).

The temperature boundary conditions are

$$T = T_s(t) \qquad \text{at} \qquad y = 0$$

$$T = T_o(t) \qquad \text{at} \qquad y = y_o$$

A linear temperature distribution was chosen as the initial condition (midnight, $t = 0$). The terms on the left hand side of the Eq. (1) represent heat conduction, radiation, diffusion of vapor water and liquid water, and the heat source/sink due to water adsorption/desorption within the insulation, respectively; whereas the term on the right hand side represents the transient term.

Radiative Transport Equation

The radiative heat flux, q_r, is required for solving Eq. (1); it is obtained by solving the radiative transport equation as presented below. The one-dimensional axially symmetric radiative transport equation for an absorbing, emitting, and anisotropically scattering medium from Ref. [13] can be written as

$$\mu \frac{dI(\tau,\mu)}{d\tau} = -I(\tau,\mu) + \frac{\omega}{2} \int_{-1}^{1} I(\tau,\mu') \, \Phi(\mu,\mu') \, d\mu' + n^2(1-\omega) \, I_b(T(\tau)) \qquad (2)$$

Here, τ ($\tau = \beta y$ and β is the extinction coefficient) is the optical depth, μ is the cosine of the polar angle Θ, ω is the single scatter albedo, n is the refractive index of the medium, $I(\tau, \mu)$ is

the radiative intensity at depth τ in the specified direction of μ, I_b is the emitted radiative intensity at depth τ, $\Phi(\mu, \mu')$ is the scattering function or phase function; here $\Phi(\mu, \mu')=1$ for isotropic scattering.

The boundary conditions for the Eq. (2) are given by

$$I(0,\mu) = \rho_s I(0,-\mu) + (1-\rho_s)n^2 I_b(T_s), \qquad \mu > 0$$
$$I(\tau_o,-\mu) = \rho_n I(\tau_o,+\mu) + (1-\rho_n)n^2 I_b(T_R), \quad \mu > 0$$

where $I_b(T_R)=e_b(T_R)/\pi$ and for a gray body $e_b(T_R)=\sigma T_R^4$. Here, ρ_s is the reflectivity of the substrate and ρ_n is the reflectivity of the roof for the no radiant barrier case. When a radiant barrier is used then ρ_n is the reflectance (.95) of the foil and T_R is the top of the batt temperature T_o. It should be noted that $n=1$ for this problem since the insulation is considered to be a stagnant layer of air with the glass fibers suspended within the air matrix and for air $n=1$. An analytical technique with the method of discrete ordinates, employing a 16 point Gaussian quadrature, was used in solving the radiative transport equation (Eq. (2)) and the details can be found in Refs. [8,13,14]. The radiative heat flux needed in Eq. (1) is given by definition as

$$q_r(\tau) = \int_0^{2\Pi} \int_{-1}^{1} I(\tau,\mu)\mu d\mu d\psi \tag{3}$$

Equations for Moisture Transport

For one-dimensional moisture transport, the liquid water conservation equation can be expressed as

$$\frac{\partial m_b}{\partial t} - \frac{\partial}{\partial y}\left[\gamma_b \frac{\partial m_b}{\partial y}\right] = \dot{m}_b \tag{4}$$

Similarly, the vapor water conservation equation can be written as

$$\frac{\partial m_v}{\partial t} - \frac{\partial}{\partial y}\left[\gamma_v \frac{\partial m_v}{\partial y}\right] = \dot{m}_v \tag{5}$$

In the above two equations, most of the terms have been defined in discussing Eq. (1). The source terms ($\dot{m}_b$, $\dot{m}_v$) in Eqs. (4) and (5) account for water adsorption/desorption. Since hysteresis is disregarded the source term is given by

$$\dot{m}_b = -\dot{m}_v = \rho_f \frac{\partial X}{\partial t} \tag{6}$$

where

$$\frac{\partial X}{\partial t} = m_\phi \frac{\partial \phi}{\partial t} \tag{6a}$$

In Eq. (6a), m_ϕ is a constant obtained from the data presented in Ref. [15] and is given in Table 1. The symbol ϕ is relative humidity and Eqs. (6) and (6a) yield the moisture adsorption/desorption as a function of the relative humidity in accordance with Ref. [16] which, for mineral fiber insulation, reported the adsorption isotherm to be a function of relative humidity only and not a separate function of temperature. The quantity X is dimensionless and has units of kg water/kg dry fiberglass. The boundary conditions for Eqs. (4) and (5) are given by

$$m_b = (m_b)_s(t); \quad m_v = (m_v)_s(t) \quad \text{at} \quad y = 0$$

$$m_b = (m_b)_o(t); \quad m_v = (m_v)_o(t) \quad \text{at} \quad y = y_o$$

where $(m_b)_s(t)$, $(m_v)_s(t)$ are the mass concentrations of liquid water and vapor water at the substrate; $(m_b)_o(t)$, $(m_v)_o(t)$ are the mass concentrations of liquid water and vapor water at the

top of the insulation batt; these concentrations were determined from the measured relative humidity and dry-bulb temperature at the substrate and top of the insulation batt. Linear vapor water and liquid water concentration profiles were chosen as the initial concentration conditions (midnight, t=0). The total heat flux is given by the following equation

$$\hat{q}_T = -k\frac{\partial T}{\partial y}\Big]_{y=0} + q_r(0) - \gamma_v\frac{\partial m_v}{\partial y}\, i_v\Big]_{y=0} - \gamma_l\,\frac{\partial m_l}{\partial y}\, i_l\Big]_{y=0} \qquad (7)$$

where the first term is the conduction term, the second the radiation term, the third the diffused vapor term, and the fourth the diffused liquid term.

Solution Scheme

Equations (1) through (6a) were solved simultaneously by an iterative scheme that employs a control volume based finite difference method (Patankar method [17]); for this problem Patankar's method becomes the same as a standard finite difference scheme. The transient solution is obtained by marching forward in time with an appropriate time step (5 min time step). The largest time step that yielded no change in the converged temperatures and species was considered the appropriate time step. A non-uniform grid with 17 nodal points (y/y_o=0, 0.003, 0.01, 0.04, 0.1, 0.2, 0.4, 0.6, 0.7, 0.8, 0.9, 0.95, 0.97, 0.98, 0.99, 0.9967, 1.00) was used in the program to achieve lower computational time without sacrificing accuracy [11]; the computation time on an IBM 3084 to predict all the results for a 24 hour period was about 60 seconds of CPU time. It should be noted that the experimental data obtained were recorded every 15 minutes and hence a linear interpolation was used to input boundary condition information at the 5 min time step intervals which occur in between the 15 minute data acquisition intervals for experimental data. A computational model was used to generate results

for all three insulation thicknesses and comparisons were made to the measured heat flux data. The model has the capability of including or excluding the moisture transport terms in the energy equation, Eq. (1). When the moisture transport terms are included, this is referred to as the "moist-case". Likewise, when the moisture transport terms are excluded, this is referred to as the "dry-case".

RESULTS

The results focus on the comparison of the total heat transfer through R-11, R-19 and R-30 insulation thicknesses and also on R-30 both with and without a radiant barrier. Radiant barrier results are based only on R-30 insulation due to the fact that a previous work [3] has already investigated R-19 insulation with and without a radiant barrier. This investigation differs from the previous work [3] by the fact that data were collected for all three insulation resistances (R-11, R-19, R-30). Due to space limitations only typical summer and winter results are depicted in this paper (data however were also collected for spring and fall conditions). These results are separated into summertime (July 6 and 15,1993) and wintertime (March 13, 1993) comparisons.

Summer Conditions

The representative summer conditions correspond to the data recorded during the 24-hour time period of July 15, 1993. Shown in Fig. 3 is the temperature-time history for the R-30 fiberglass insulation batt with a radiant barrier. Similar temperature histories were measured for the R-30 fiberglass insulation batt without a radiant barrier and for other insulation thicknesses (R-11 and R-19 without a radiant barrier) but are not shown here due to space

limitations. The roof temperatures, top of the batt temperatures, and bottom of the batt temperatures are all employed as boundary condition information in the computational model. This was a typical partly cloudy day exhibiting a dip in the peak of the roof temperature (T_R) profile. The roof temperature is seen to reach a high value, hence the roof radiates a high heat flux onto the insulation batt that is covered by a radiant barrier. The radiant barrier reflects the radiative heat flux incident from the roof back into the attic air space, resulting in the top of the insulation temperature (T_o) remaining lower than the attic air (T_A) temperature. If this would have been a batt without a radiant barrier, the top of the batt temperature (T_o) would be higher than the attic air temperature (T_A) (measured at 0.051 m above the batt).

Shown in Fig. 4 are the dimensionless vapor water concentration histories for the R-11, R-19 and R-30 insulation batts without a radiant barrier. It can be seen from Fig. 4 that for 7/15/92 the vapor concentration at the top of the batt is always greater than at the substrate for all three cases; hence there was a diffusion of vapor water from the top to the bottom of the batt. The bulk concentration gradient across the batt increases somewhat as the insulation thickness increases. The vapor concentration is significantly higher at the top of the batt during the high temperature portion of the day; this is due to water desorption both from the attic wooden structural components such as roofing boards and also due to desorption from the attic insulation binder. Shown in Fig. 5 are the vapor water concentration histories for the R-30 (for 7/6/93) fiberglass insulation batt with and without a radiant barrier. The profiles are similar to those of Fig. 4. In comparing the two cases (with and without a radiant barrier) it can be seen that the bulk vapor concentration gradient across the batt decreases when a radiant barrier is employed. Once a radiant barrier is employed, diffusion through the top of a batt occurs

because the barrier is perforated which allows the transport of vapor through the porous radiant barrier. Even though the radiant barrier is perforated, the vapor water is still somewhat retarded from diffusing from the high concentration vapor water attic air through the radiant barrier and into the insulation batt. Hence, the vapor concentration is greater at the top of the batt for the no radiant barrier case.

Figure 6 depicts the various components of the total heat transfer: radiation, conduction and vapor water and liquid water mass transport for R-19 insulation. For the dry case, conduction through the insulation batt accounted for 60 percent of the total heat transfer; while the radiation accounted for about 40 percent of the total heat transfer. For the moist case, conduction accounted for 50 percent of the heat transfer; radiation accounted for about 25 percent of the heat transfer; while the mass transport accounted for about 25 percent of the total heat transfer. The combination of all three components make up the total heat transfer.

The information shown in Figs. 3 and 4 was employed as the boundary conditions for the vapor water species equation (Eq.(5)). The liquid water concentration is essentially the same as given by Eq. (6a) since the liquid water conductivity coefficient is very small (see Table 1). With the measured temperatures and concentrations employed as boundary condition information, the predicted total heat flux (Eq.(7)) for R-11, R-19, and R-30 insulations were compared to the respective measured heat flux data for cases without a radiant barrier as shown in Fig. 7. Presented in Fig. 7 are the experimental data for R-11, R-19 and R-30. It can be seen that in general there is good agreement between the experimental data and the predicted heat fluxes for all three insulations which is later quantified in Table 2. During the heating portion of the day it can be seen that the heat flux level is greater in magnitude (i.e. more negative) for the

R-11 insulation indicating that the thinner insulation, R-11 (0.089 m thick), allows more heat transport into the house. The R-19 insulation (0.158 m thick) predictions and data fall between that of the R-11 and R-30 insulations. The R-30 insulation (0.247 m thick) has the lowest heat flux level, hence allowing the least amount of heat transfer into or out from the house. Table 2 shows the integrated heat fluxes for the measured data and for the predicted dry and moist case situations for all three insulation thicknesses (R-11, R-19, and R-30). When a comparison is, made for R-30 insulation, it can be seen that the moist case scenario agrees quite well with the experimental data (5.7%). It is also seen in Table 2, that when moisture is present in the system, the total heat flux increases by approximately 12%-27% for all three insulations without a radiant barrier for summer conditions, as compared to predicted dry conditions.

The R-30 insulation batt resulted in acceptable magnitudes of heat transfer on July 15, 1993, however, a day with an even higher flux level (July 6, 1993) is used to better illustrate the effects of radiant barriers for the R-30 insulation. Shown in Fig. 8 is the comparison of the substrate heat flux for R-30 insulation with and without a radiant barrier for July 6, 1993. For summer conditions, Table 2 shows that without a radiant barrier the predicted integrated heat fluxes agree well with the experimental data for all three cases; 11.2% for R-11, 3.1% for R-19, and 6.5% for R-30. For both the measured and the predicted heat fluxes, the overall heat transfer decreased considerably when a radiant barrier was employed. Using the R-30 insulation batt without a radiant barrier as the standard, Table 2 shows that the integrated heat fluxes decreased by about 27% once a barrier was implemented. This can be explained by the fact that when a radiant barrier is present the radiative heat flux from the roof is reflected back into the attic, thus not allowing heat to be transferred into the house. Therefore, the total heat flux

will significantly decrease by 27% once a radiant barrier is employed.

Winter Conditions

The data recorded during the 24-hour time period of March 13, 1993 was representative of typical northern Mississippi winter conditions. The temperature-time histories are shown in Fig. 9 for the R-30 insulation without a radiant barrier. This was a winter day with the ambient temperature reaching a high of only 273 K ($\approx$ 32 F). The roof temperatures are the lowest during the early morning hours ($t < 400$ min) but increase rapidly during the day as a result of solar heating. The attic air (T_A) and top of the batt (T_o) temperatures remain lower than the bottom of the insulation (T_s) temperature during most of the day. This indicates that heat would be lost (positive heat flux) during the corresponding portions of the day. Similar temperature histories were observed for the case with a radiant barrier but are not shown due to paper space limitations.

The bulk vapor water concentration gradients across the batts for all three insulation thicknesses were found to be essentially zero. Figures 10 and 11 illustrate this fact by showing the heat flux comparisons of the moist and dry cases for the three thicknesses. Figure 10 shows the comparisons of the dry and the moist cases for R-11, R-19 and R-30 all without a radiant barrier. From Fig. 10 it can be seen that there is only a slight difference between the dry and moist cases with the moist cases being slightly higher. If there would have been a significant vapor water concentration difference between the top and the bottom of the fiberglass batt, then there would have been a significant difference between the dry case and moist case heat flux predictions. The greater the bulk concentration gradient across the batt, the greater the moisture transport through the insulation batt. The vapor water transports enthalpy as it diffuses through

the batt causing an increase in the overall heat transfer at the substrate. Table 2 shows that without a radiant barrier the predicted integrated heat fluxes agree with the experimental data as follows; 9.8% for R-11, 5.2% for R-19, and 39.6% for R-30. The agreement between the experimental data and predictions for R-11 and R-19 is considered to be good. The agreement for R-30 on a percentage basis is not as good because of the low flux levels that are associated with the R-30 fiberglass insulation. Table 2 also shows that there is an integrated heat transfer difference of only 1.2% between the moist and dry cases for R-11, 6.4% for R-19 and 7.3% for R-30. This illustrates how the overall heat transfer increased for the three insulation batts when moisture was present. Similar conclusions can be reached from Fig. 11, which shows the comparison of the dry and moist heat transfer cases for R-30 insulation with and without a radiant barrier. For both the cases with and without a radiant barrier, the difference between the dry and moist cases are very small with the moist case being slightly higher. This would indicate that the overall heat transfer increased very slightly with moisture being present even when a radiant barrier was employed for winter conditions.

Figure 12 further illustrates the effects of moisture being present. Figure 12 shows the predicted substrate heat flux histories for the conduction, radiation, vapor water and liquid water conductivity components with and without the presence of moisture. From Fig. 12 it can be seen that the dry case radiation and conduction components are slightly higher than the moist case radiation and conduction components. Hence, the total heat fluxes are higher for the moist case due to mass diffusion (primarily vapor water) and to water adsorption and desorption.

Illustrated in Fig. 13 are the total heat fluxes corresponding to the R-11, R-19 and R-30 experimental data and the predictions from the numerical moist case for R-11, R-19, and R-30

for the case without a radiant barrier. Throughout the entire day the R-11 insulation displays higher heat fluxes (positive sign) indicating more heat is leaving the house. The R-19 insulation has a similar trend; heat is leaving the house but at a lower heat flux than the R-11. As expected the R-30, thickest of the insulations, demonstrates the lowest heat fluxes, hence allowing the least amount of heat to escape from the house. Table 2 presents a comparison of the integrated heat fluxes for the three insulations without a radiant barrier for both dry and moist cases. For these winter conditions, the presence of moisture is computed to have a very small effect on the overall heat flux for all three thicknesses.

Comparison of R-30 insulation heat flux data for both the radiant barrier and no radiant barrier cases showed no significant difference for winter conditions. Hence, due to paper limitations no figure will be shown to support this non-effect; this does agree with the winter-time conclusion of Ref. [7]. However, for summer conditions the radiant barrier was found to be quite effective for R-30 (27% reduction).

CONCLUSIONS

The effects of varying the thickness from R-11 to R-19 to R-30 for attic insulations without a radiant barrier and R-30 with a radiant barrier have been investigated in this study. As expected, the increased thickness from R-11 to R-19 to R-30 did decrease the total amount of heat flux which enters or leaves the occupied living space depending on the climatic conditions. The computational model was able to predict results with and without the moisture transport terms included. With the presence of moisture, the total heat flux was increased significantly for all summertime cases. Therefore, it has been found in this study as well as in previous works [3-4], that moisture is detrimental to energy conservation for summer conditions

by increasing the total heat flux which enters the occupied living space. Whereas, for wintertime conditions moisture was found to be slightly detrimental in affecting the total heat transfer. The addition of a horizontal radiant barrier to the insulation top surface decreased the total heat flux significantly for the R-30 insulation for summer conditions. This study found that for summer conditions (R-30) a decrease of 27% in total heat transfer with the addition of a radiant barrier. Winter results for R-30 showed the addition of a radiant barrier to have no significant effect. These results have concluded that with the presence of moisture in an attic system the total heat transfer will be increased or decreased into the household depending on whether it is winter or summer climatic condition. Likewise, those households that have high efficiency fiberglass insulation (i.e. R-30) can achieve even higher efficiency levels with the addition of radiant barriers.

ACKNOWLEDGEMENT

The authors wish to acknowledge the support of the Department of Energy EPSCoR program sponsored under grant number DE-FG02-91ER75660. Also the authors would like to acknowledge the support of the National Science Foundation for the equipment purchased under award number 8905471.

REFERENCES

[1] Levins, W.P., Karnitz, M.A., and Hall, J.A., "Moisture Measurements in Single-Family Houses with Attics Containing Radiant Barriers", Oak Ridge National Laboratory, Report ORNL/CON-255, February 1989.

[2] Gorthala, R., Roux, J. A. and Fairey III, P. W.,"Combined Conduction, Radiation Heat

Transfer and Mass Transfer in Fibrous Attic Insulations," Insulation Materials: Testing and Applications, 2nd Volume, ASTM STP 111, American Society for Testing and Materials, Philadelphia, 1991, pp. 371-386.

[3] Harris, K.T., McCarty, T.A., Roux, J.A., and Gorthala, R., "Total Heat Transfer Due to the Variation in Fiberglass Insulation Thickness in Attics," ASME National Conference on Heat Transfer, August 8-11, 1993, Radiative Heat Transfer Theory and Applications, HTD-Vol. 244, pp. 1-10.

[4] Gorthala, R., Harris, K.T., Roux, J.A., and McCarty, T.A., "Transient, Conductive, Radiative Heat Transfer Coupled with Moisture Transport in Attic Insulations," Journal of Thermophysics and Heat Transfer, to be published in Vol. 7, No. 4, Oct.-Dec. 1993.

[5] Levins, W.P. and Karnitz, M.A., "Cooling-Energy Measurements of Unoccupied Single-Family Houses with Attics Containing Radiant Barriers," Oak Ridge National Laboratory, Report ORNL/CON-200, July 1986.

[6] Levins, W.P. and Karnitz, M.A., "Heating Energy Measurements of Unoccupied Single-Family Houses with Attics Containing Radiant Barriers," Oak Ridge National Laboratory, Report ORNL/CON-213, January 1987.

[7] Levins, W.P. and Karnitz, M.A., "Heating Energy Measurements of Single-Family Houses with Attics Containing Radiant Barriers in Combination with R-11 and R-30 Ceiling Insulation," Oak Ridge National Laboratory, Report ORNL/CON-239, August 1988.

[8] Tao, Y.-X., Besant, R. W. and Rezkallah, K. S.,"Transient Thermal Response of a Glass-Fiber Insulation Slab with Hygroscopic Effects'" Int. J. Heat Mass Transfer, Vol.

35, No. 5, May 1992, pp.1155 - 1167.

[9] Tao, Y.-X., Besant, R. W. and Simonson, C. J.,"Measurement of the Heat of Adsorption for a Typical Fibrous Insulation," ASHRAE Transactions, 1992, Vol. 98, Part II.

[10] Hust, J. G., Callanan, J. E., and Sullivan, S. A.,"Specific Heat of Insulations," Thermal Conductivity 19, D. W., Yarbrough, Ed., Plenum, N.Y., 1988, pp. 533-550.

[11] Yeh, H. Y., and Roux, J. A., "Spectral Radiative Properties of Fiberglass Insulation", Journal of Thermophysics and Heat Transfer, Vol. 2, No. 1, January 1988, pp. 75-81.

[12] Houston, R.L., and Korpela, S.A., "Heat Transfer through Fiberglass Insulation", Proceedings of the 7th International Heat Transfer Conference, Vol.2, 1982, pp. 499-504.

[13] Roux, J. A., Smith, A. M., and Todd, D. C., "Radiative Transfer with Anisotropic Scattering and Arbitrary Temperature for Plane Geometry," AIAA Journal, Vol. 13, No. 9, Sept. 1975, pp.1203-1211.

[14] Rish, J. W., and Roux, J. A.,"Heat Transfer Analysis of Fibrous Insulations With and Without Radiant Barriers for Summer Conditions," Journal of Thermophysics and Heat Transfer, Vol. 1, No. 1, January 1987, pp. 43-49.

[15] Hansen, K. K.,"Sorption Isotherms," A Catalogue, 1985, Building Materials Laboratory, Department of Civil Engineering, The Technical University of Denmark.

[16] Langlais, C., Hyrien, M., and Klarsfeld, S., "Mositure Migration in Fibrous Insulating Materials Under the Influence of a Thermal Gradient and Its Effect on Thermal Resistance," Moisture Migration in Buildings, ASTM STP 779, 1982, pp. 191-206.

[17] Patankar, S. V., Numerical Heat Transfer and Fluid Flow, Hemisphere Publishing Corp., Washington, D.C., 1980.

[18] Holman J.P., Heat Transfer, McGraw-Hill Publishing, 7th Ed., 1990

[19] Yajnik, S. and Roux, J.A., "Determination of Radiative Properties of Fiberglass and Foam Insulation", Oak Ridge National Laboratory, Report ORNL/Sub/86-55930/1, 1986.

BIOGRAPHIES

Kendall T. Harris

Mr. Harris received his M.S. degree in Engineering Science at the University of Mississippi in August, 1993. He is currently working on his Ph.D. in Mechanical Engineering in the area of heat transfer in fibrous insulation. His research interests include numerical modeling and experimental investigations. He received his B.S. in Aerospace Engineering from the University of Kansas, 1990.

Tyrus A. M°Carty

Dr. M°Carty received his B.S. degree in Mathematics and Physics (1975) from Tougaloo College, and both the M.S. (1979) and Ph.D. (1987) from the University of Mississippi. He has worked as a Research Associate for the Center of Computational Hydroscience and Engineering at the University of Mississippi and as a Research Engineer for the Corps of Engineers Waterways Experiment Station. He presently serves as an Assistant Professor of Mechanical Engineering at the University of Mississippi. His research interests are in the areas of fluid mechanics, heat transfer, and computational/numerical modeling.

Jeffrey A. Roux

Dr. Roux received his B.S. degree in Mechanical Engineering in 1967 from LSU, and both the

M.S. (1968) and Ph.D. (1970) form the University of Tennessee. He has worked in industry for 10 years (2 with Northrop, Inc. and 8 with Sverdup, Inc.) and has taught at the University of Mississippi for the past 13 years in the Mechanical Engineering Department. His 23 years of research experience are all in the thermophysics and heat transfer areas. Dr. Roux's works have ranged from aerodynamics heating, thin film optics, radiative heat transfer in fibrous insulation, solar energy to thermochemical analysis of composite materials.

LIST OF FIGURES

Fig. 1 Attic sketch
Fig. 2 Location of heat flux meters, relative humidity meters and thermocouples about the insulation batt.
Fig. 3 Temperature-time histories for R-30 fiberglass insulation with a radiant barrier.
Fig. 4 Vapor water concentration histories for R-11, R-19 and R-30 at different locations of the batt for July 15, 1993.
Fig. 5 Vapor water concentration histories for R-30 at different locations of the batt with and without a radiant barrier.
Fig. 6 Predicted substrate heat flux-time histories for the conduction, radiation, vapor and bound mass diffusion components for R-19 fiberglass insulation.
Fig. 7 Substrate measured heat flux-time histories and predicted heat flux-time histories for R-11, R-19 and R-30 insulation batts without a radiant barrier for July 15, 1993.
Fig. 8 Substrate measured heat flux-time and predicted hat flux-time histories for R-30 insulation with and without a radiant barrier.
Fig. 9 Temperature-time histories for R-30 fiberglass insulation without a radiant barrier for March 13, 1993.
Fig. 10 Predicted heat flux-time histories for R-11, R-19 and R-30 insulation batts with and without moisture present.
Fig. 11 Predicted heat flux-time histories for R-30 insulation batts with and without a radiant barrier and moisture present.
Fig. 12 Predicted substrate heat flux-time histories for the conduction, radiation, vapor and bound mass diffusion components for R-19 fiberglass insulation.
Fig. 13 Substrate measured heat flux-time histories and predicted heat flux-time histories for R-11, R-19 and R-30 insulation batts without a radiant barrier for March 13, 1993.

LIST OF TABLES

Table 1 Radiative and thermal properties used in numerical computations.
Table 2 Time integrated substrate heat flux corresponding to predicted and measured R-11, R-19 and R-30 with and without a radiant barrier for summer and winter conditions.

TABLE 1. Radiative and thermal properties used in numerical computations.

ρ_f[a]	12.0	kg/m^3
c_f[a]	844.4	J/kg-K
k_f[b]	$a + bT + 8.5537 \times 10^{-5} \rho_f$ $a = 4.97576 \times 10^{-3}$, $b = 7.00025 \times 10^{-5}$	W/m-K
ω[c]	0.201	
β[c]	3.70	cm^{-1}
γ_{vR}[d]	1.2×10^{-5}	m^2/s
γ_b[e]	1.19×10^{-9}	m^2/s
m_ϕ[f]	$1/100 \quad .10 \leq \phi \leq .90$	
γ_v/γ_{vR}[d]	$(T/T_r)^{1.5}$	

[a]Ref. [10], [b]Ref. [12], [c]Ref. [19], [d]Ref. [18], [e]Ref. [8] [f]Ref. [15]

TABLE 2. Time integrated substrate heat flux corresponding to R-11, R-19, and R-30 with and without a radiant barrier and measured substrate heat fluxes for summer and winter conditions.

Date	Radiant Barrier	Case	Predictions R-11 kJ/m²		R-19 kJ/m²		R-30 kJ/m²	
7/15/93[a]	With	Moist	---		---		-31.7	(30%)[c]
		Dry	---		---		-22.1	
		Data	---		---		-29.7	[5.7%][d]
	Without	Moist	-85.3	(12%)	-56.1	(27%)	-43.8	(27%)
		Dry	-75.2		-41.1		-32.2	
		Data	-76.6	[11.2%]	-57.9	[3.1%]	-41.1	[6.5%]
3/13/93[b]	Without	Moist	180.8	(1.2%)	109.8	(6.4%)	77.2	(7.3%)
		Dry	178.6		102.8		71.5	
		Data	164.6	[9.8%]	104.3	[5.2%]	55.3	[39.6%]

[a]Integrated over heat gain period (530 min < t < 1410 min)

[b]Integrated over heat loss period (24 hours)

[c]Numbers in parenthesis represent the difference between the moist case and dry case with the moist case being the standard.

[d]Numbers in the brackets represent the difference between the experimental data and the moist case with experimental data being the standard.

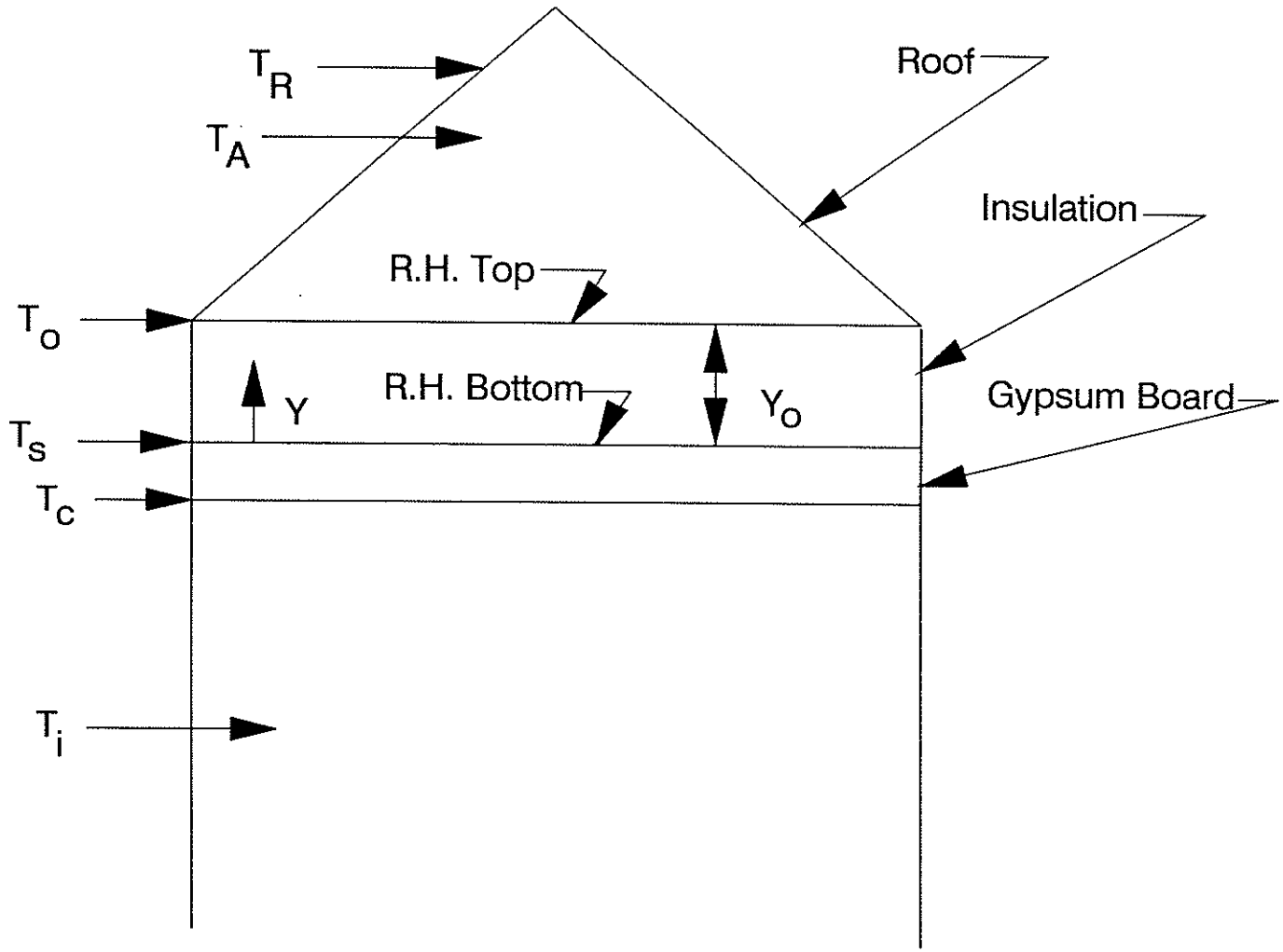

Fig. 1 Attic sketch.

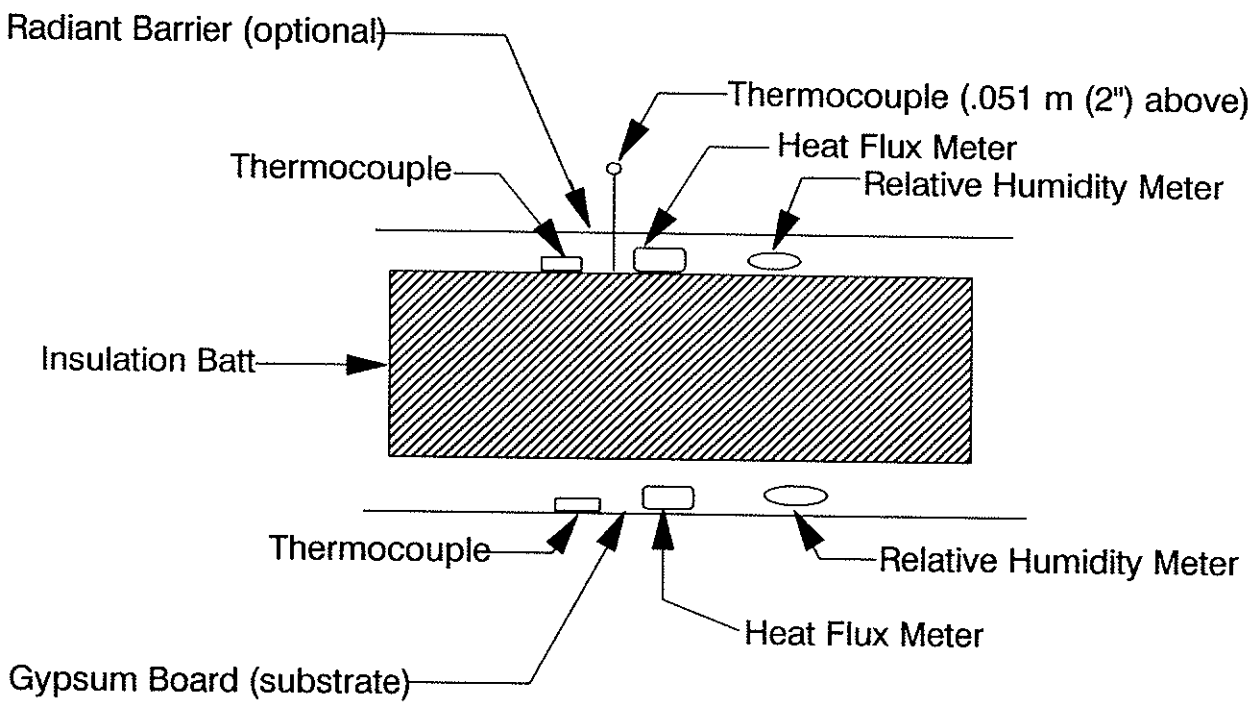

Fig. 2 Location of heat flux meters, relative humidity meters and thermocouples about the insulation batt.

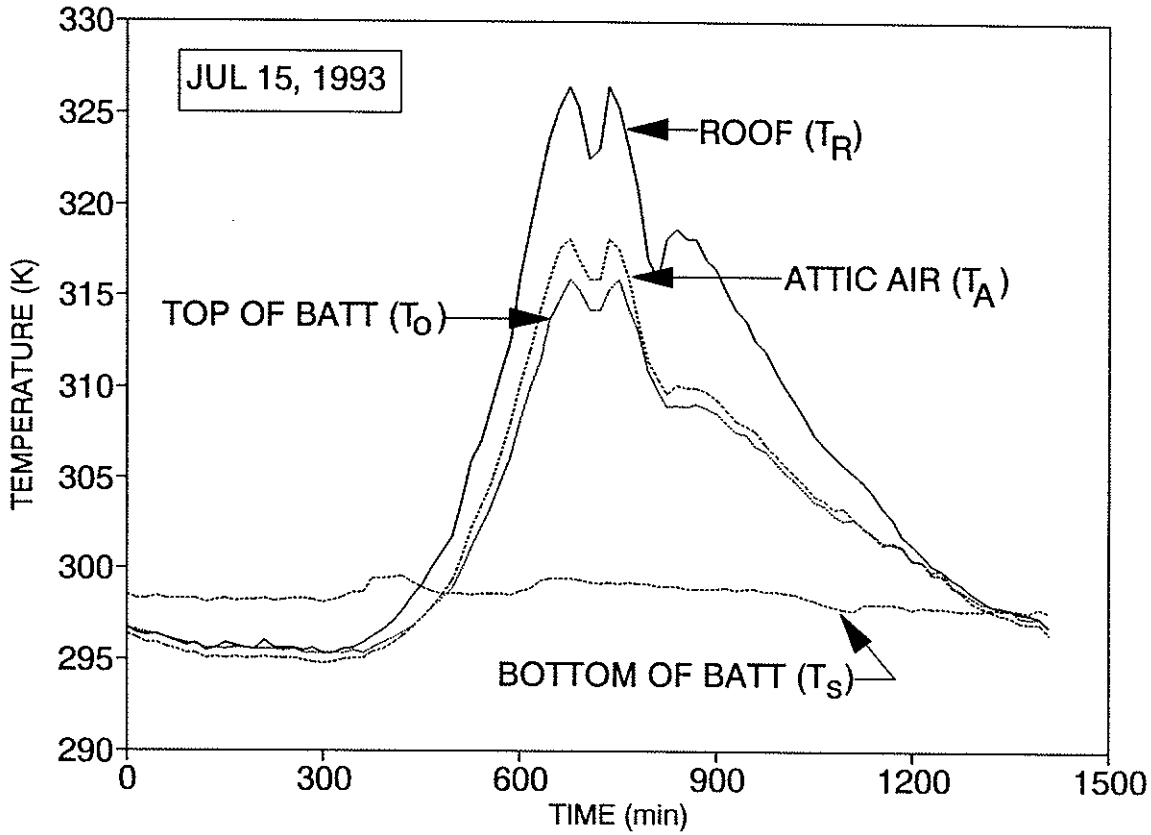

Fig. 3 Temperature-time histories for R-30 fiberglass insulation with a radiant barrier for July 15, 1993.

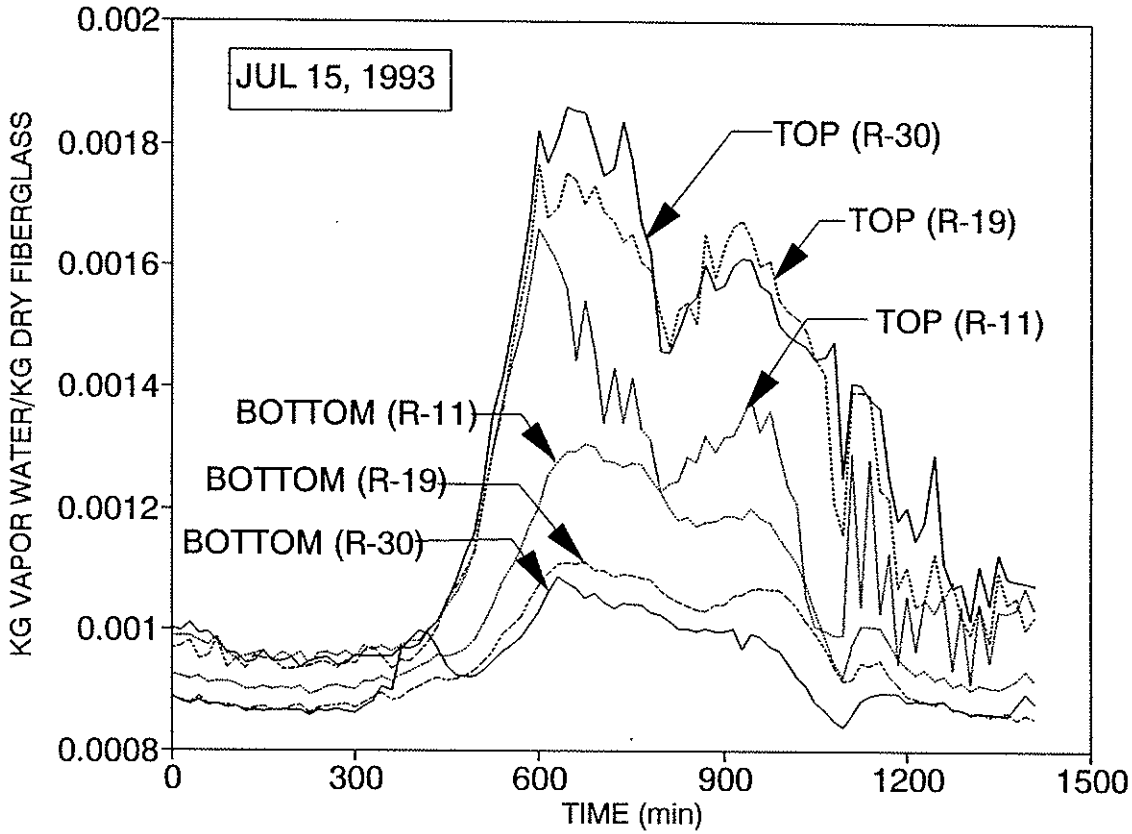

Fig. 4 Vapor water concentration histories for R-11, R-19, and R-30 at different locations of the batt for July 15, 1993.

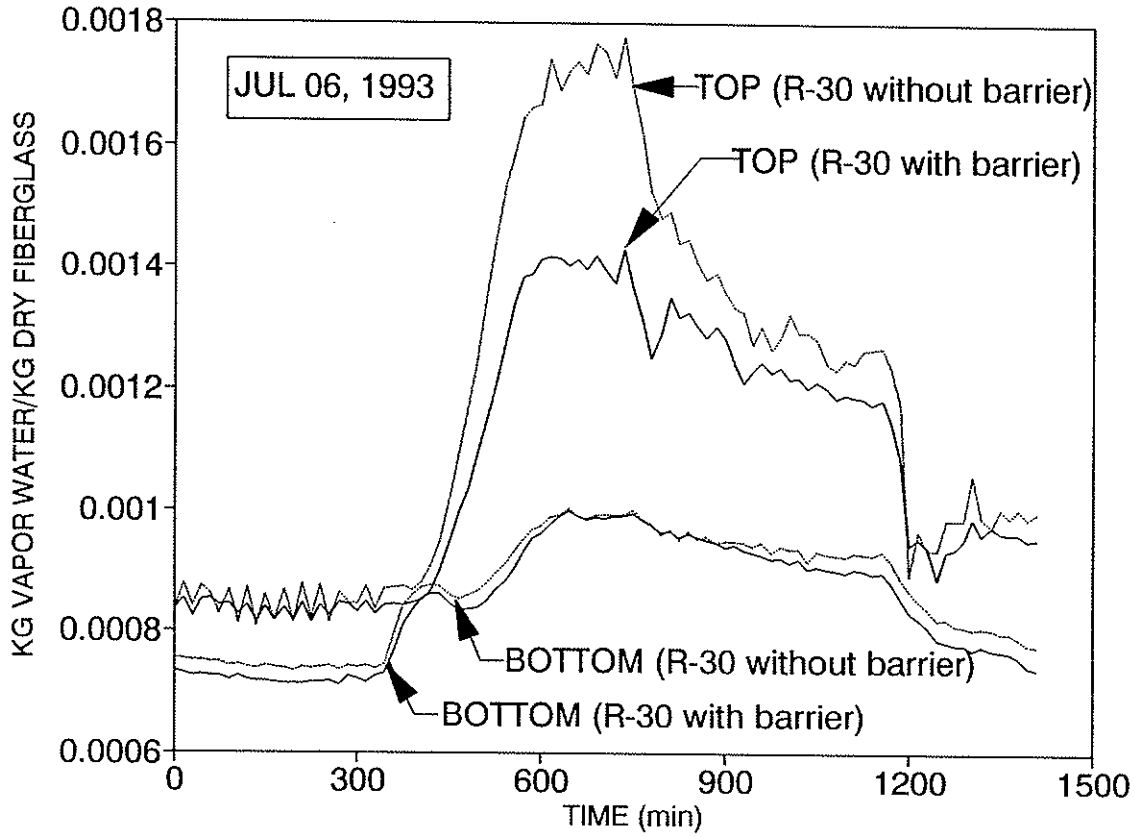

Fig. 5 Vapor water concentration histories for R-30 at different locations of the batt with and without a radiant barrier.

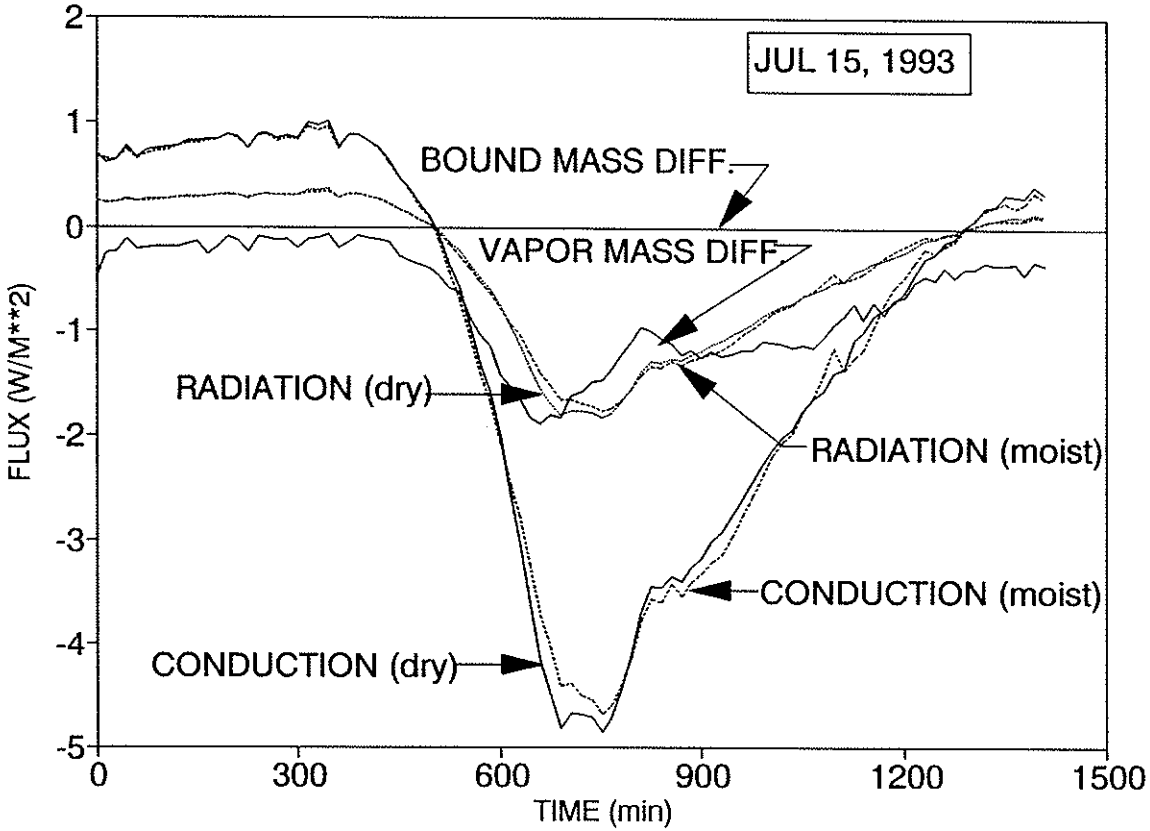

Fig. 6 Predicted substrate heat flux-time histories for the conduction, radiation, vapor and bound mass diffusion components for R-19 fiberglass insulation.

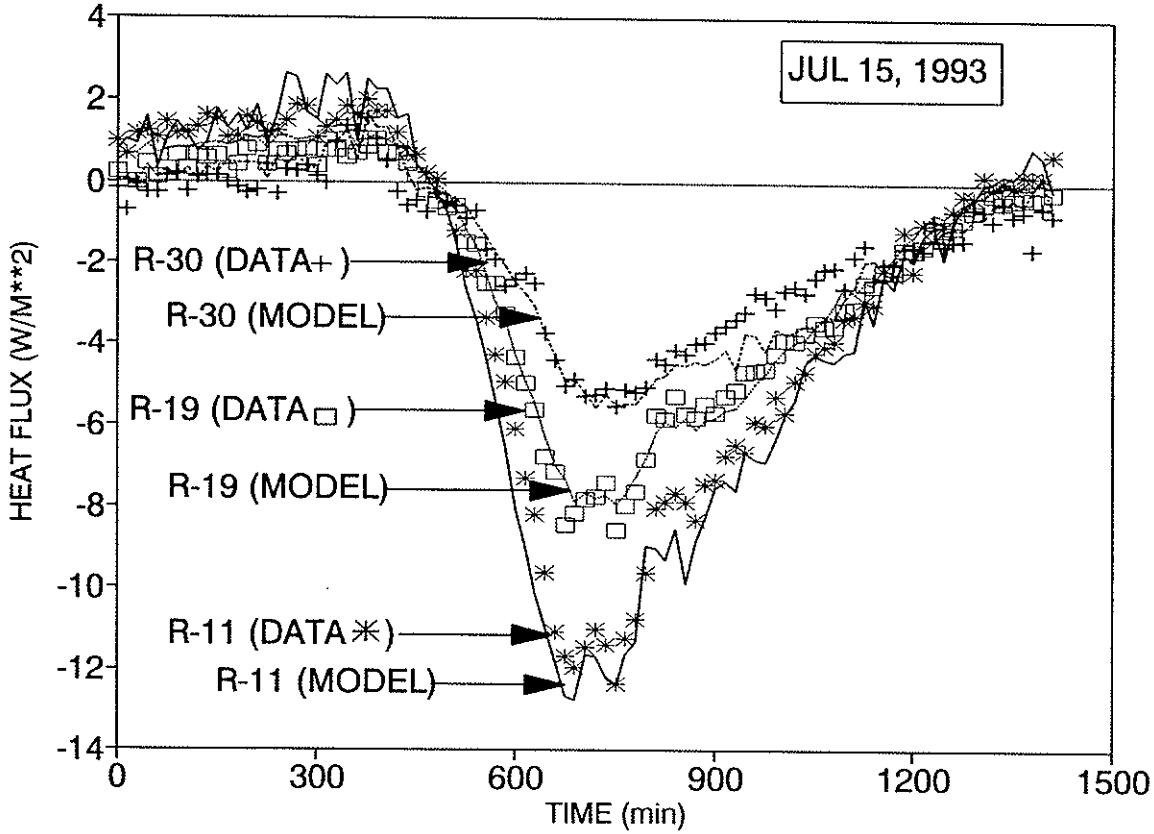

Fig. 7 Substrate measured heat flux-time histories and predicted heat flux-time histories for R-11, R-19 and R-30 insulation batts without a radiant barrier for July 15, 1993.

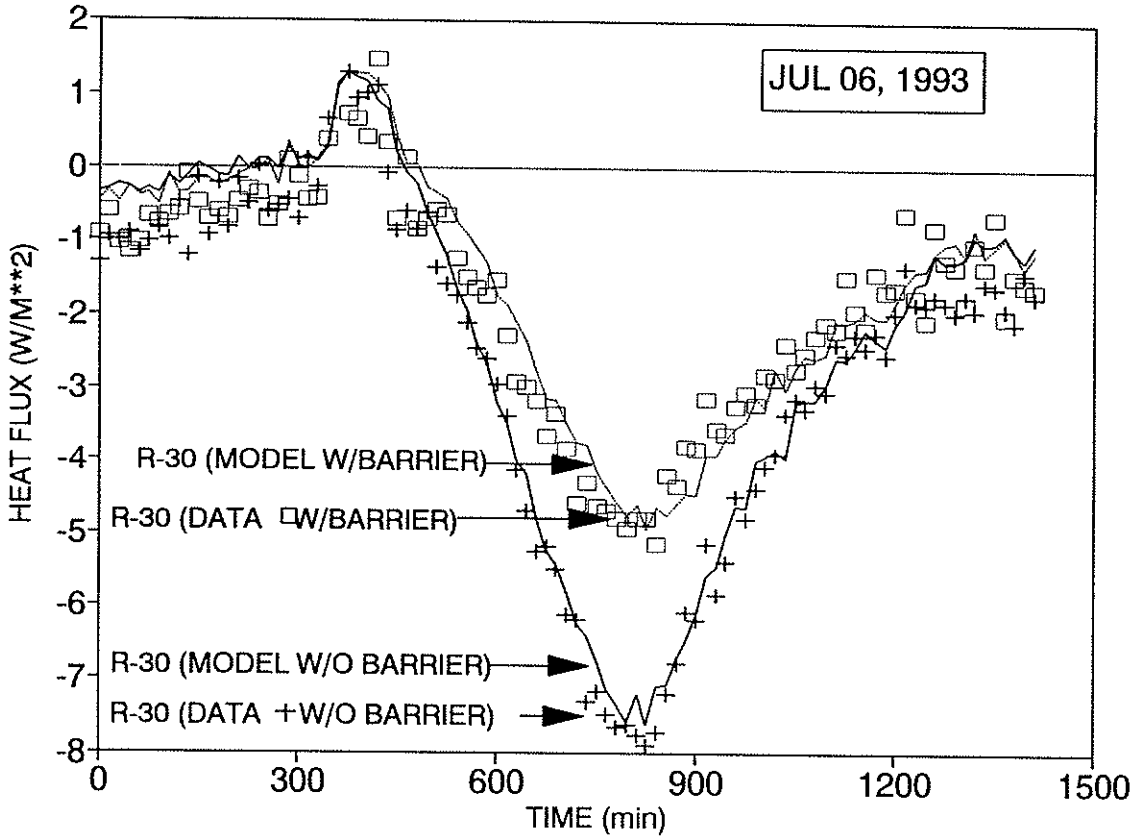

Fig. 8 Subsrtate measured heat flux-time and predicted heat flux-time histories for R-30 insulation with and without a radiant barrier.

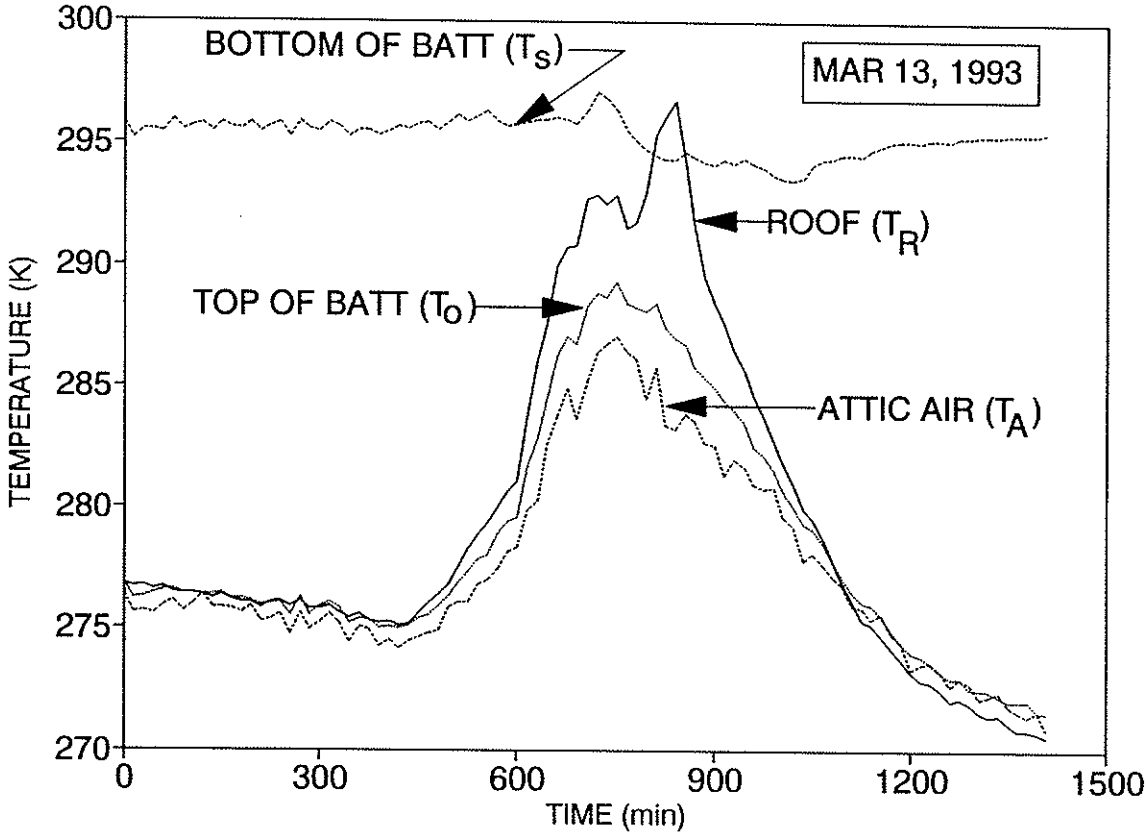

Fig. 9 Temperature-time histories for R-30 fiberglass insulation without a radiant barrier for March 13, 1993.

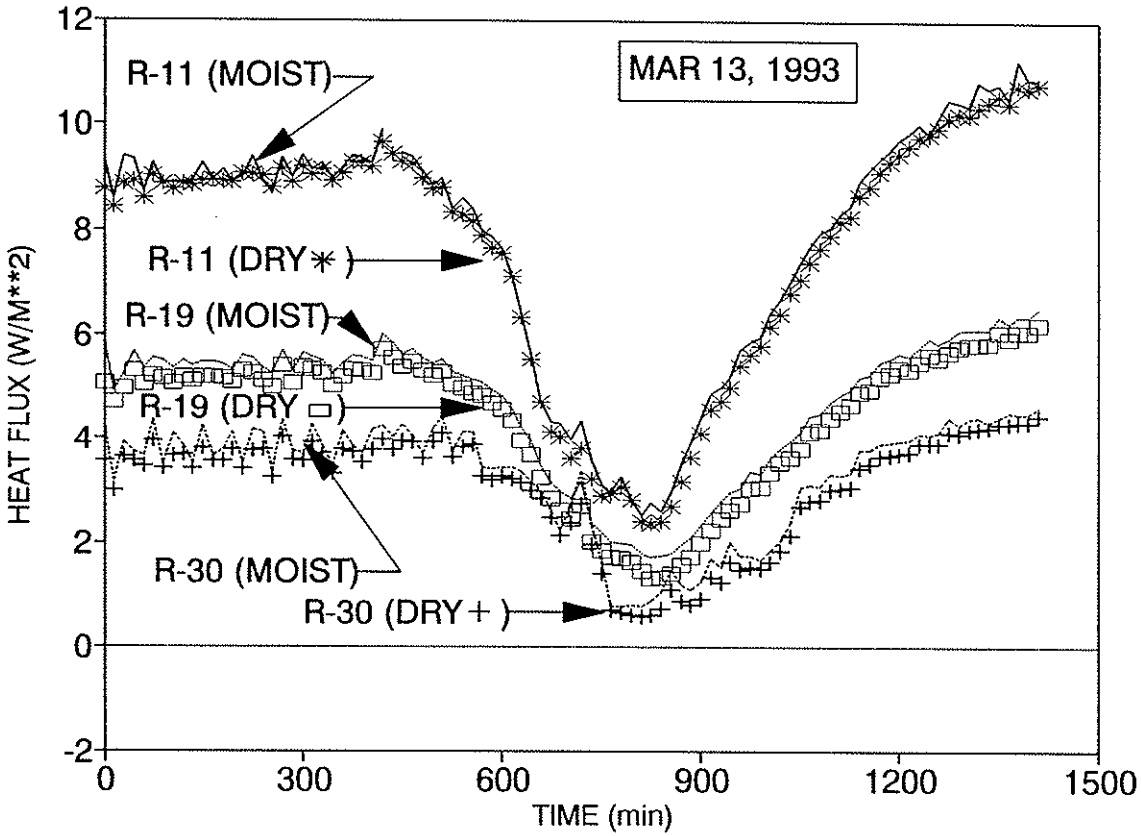

Fig. 10 Predicted heat flux-time histories for R-11, R-19 and R-30 insulation batts with and without moisture present.

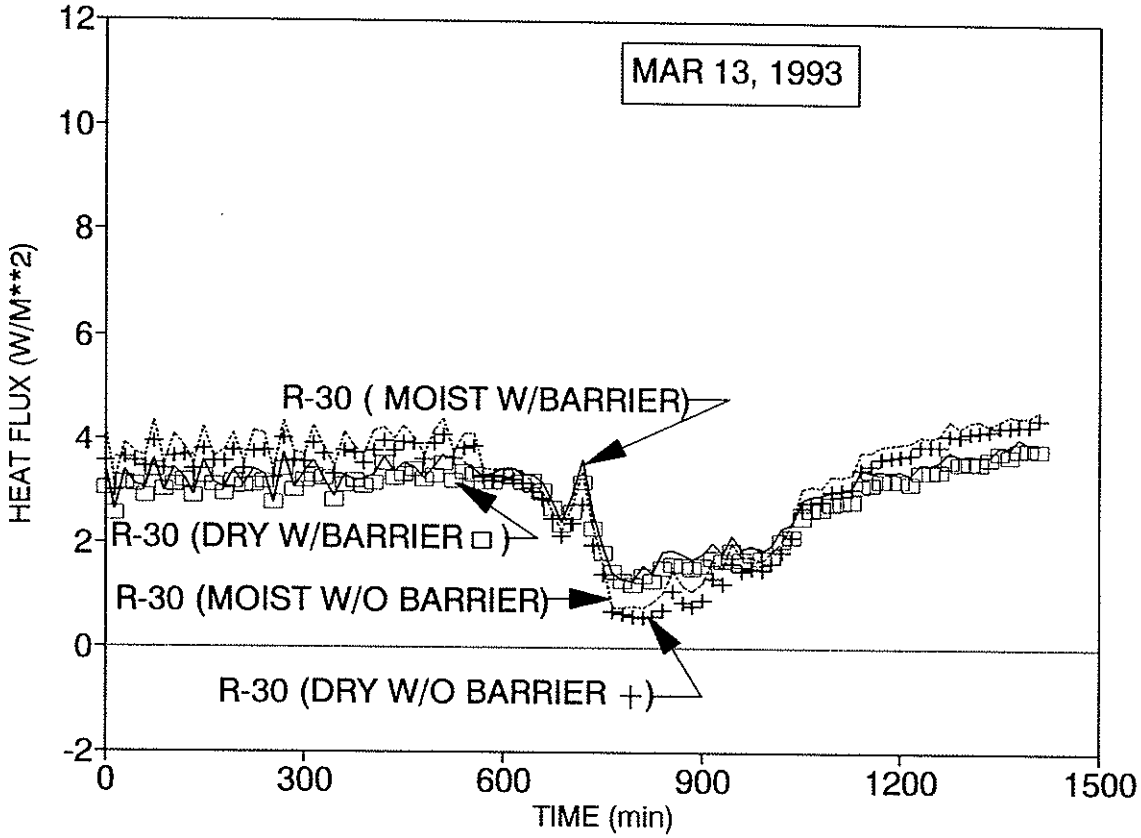

Fig. 11 Perdicted heat flux-time histories for R-30 insulation batts with and without a radiant barrier and moisture present.

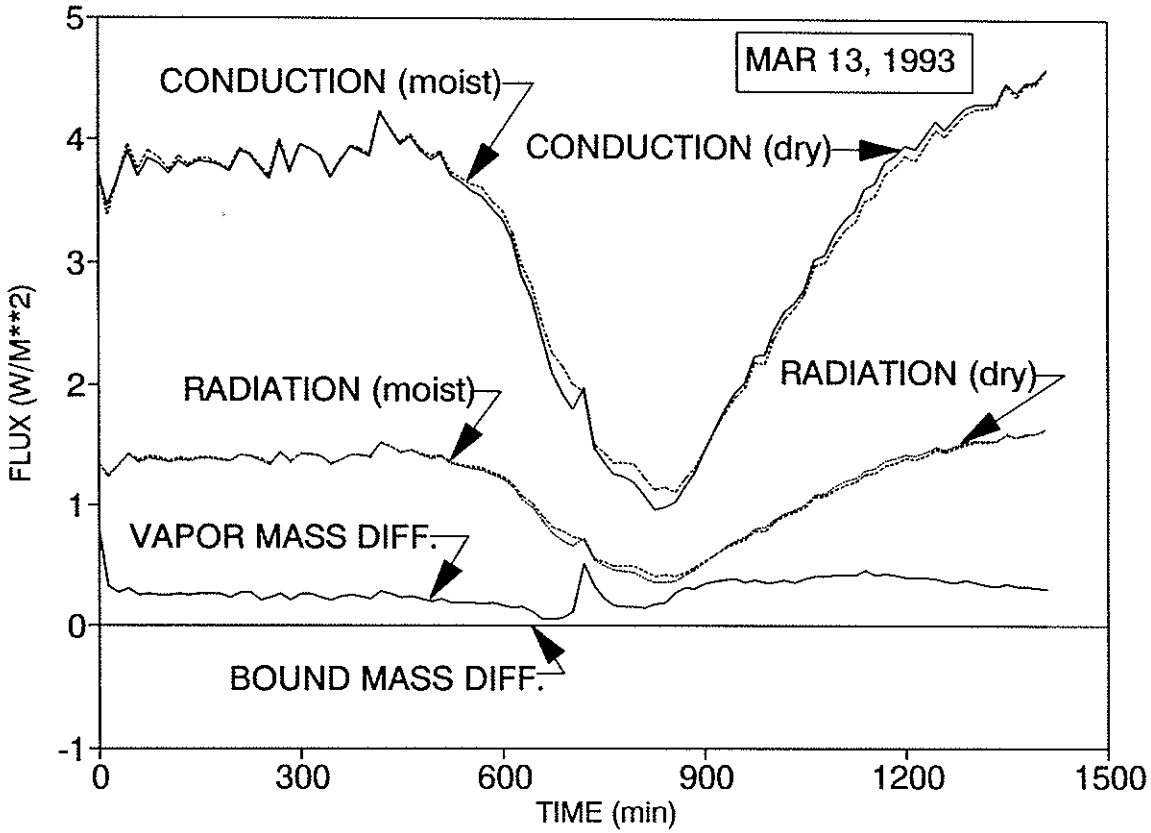

Fig. 12 Predicted substrate heat flux-time histories for the conduction, radiation, vapor and bound mass diffusion components for R-19 fiberglass insulation.

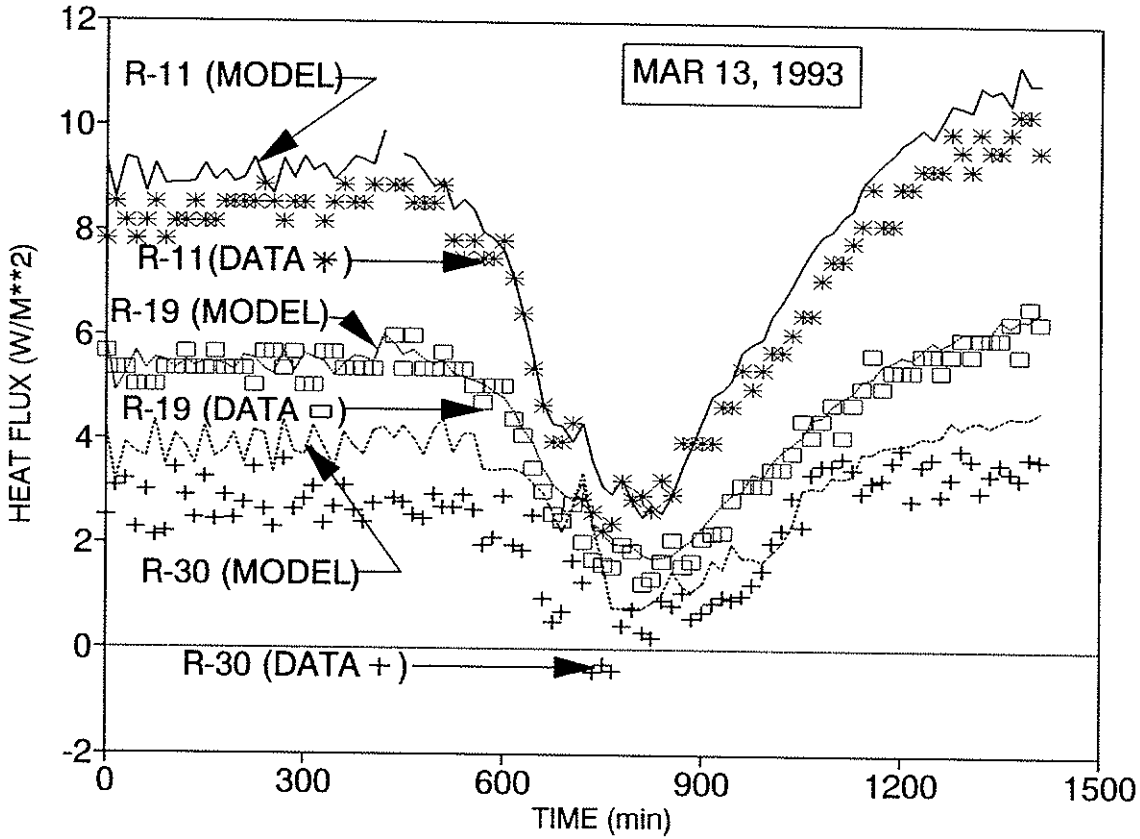

Fig. 13 Substrate measured heat flux-time histories and predicted heat flux-time histories for R-11, R-19, and R-30 insulation batts without a radiant barrier for March 13, 1993.